

Supporting Information

for

Influence of Current Collector Materials on the Electrochemical Performance of Aqueous Zinc-Ion Batteries

Iman P. Pinnock,¹ Yujia Fan,¹ Ivan P Parkin,^{2,*} Buddha Deka Boruah^{1,*}

¹Institute for Materials Discovery (IMD), University College London (UCL), London WC1E
7JE, UK

²Department of Chemistry, University College London (UCL), London WC1H 0AJ, UK

Corresponding authors: Prof. Ivan P. Parkin: i.p.parkin@ucl.ac.uk

Dr. Buddha Deka Boruah: b.boruah@ucl.ac.uk

Supplementary Results

Figure S1a and **b** displays SEM images of VO₂ (B) nanorods fabricated via hydrothermal synthesis, at different magnifications. Flaky VO₂ (B) rods can be seen in **Figure S1a** clustered together, which is further highlighted in **Figure S1b** as at the higher magnification you can see the individual nanorods within the cluster.

A Raman spectrum of the material was obtained (**Figure S1c**), from which all the expected Raman peaks were visible.^{1,2} The peaks at 140.9 cm⁻¹ and 190.8 cm⁻¹ correspond to the layered lattice structure. The peaks at 281.5 cm⁻¹ and 405.8 cm⁻¹ are attributed to V=O bending vibrations, while the 688.5 cm⁻¹ peak arises from the V–O–V stretching mode associated with corner-shared oxygens of two pyramids. The 990.6 cm⁻¹ peak is assigned to the stretching vibration of the terminal V=O bond.¹

X-ray diffraction measurements were taken to further ensure the correct material has been synthesised. The XRD spectra (**Figure S1d**) for the VO₂ (B) nanorods produced the expected peaks, with the corresponding planes indicated, when compared to the MDI Jade XRD data base. The characteristic peaks for VO₂ (B) are observed at $2\theta = 14.4^\circ, 15.4^\circ, 25.4^\circ, 29.0^\circ, 30.2^\circ, 44.2^\circ, 45.1^\circ, \text{ and } 49.5^\circ$, corresponding to the (001), (200), (110), (002), (-401), (003), (-601), and (020) Miller indices, respectively.³ These are the strong peaks, with every peak intensity being above 5, which coupled with the presence of the two peaks at 14° and 15° (approx.), confirm that the material is VO₂ (B). The desired phase was successfully achieved, as every peak with an intensity above 5 is present and the characteristic peaks at approx. 14° and 15° are clearly visible, confirming that B phase has been synthesised as these peaks are absent in XRD spectra of other VO₂ (B) phases.⁴ Moreover, there was no V₂O₅ left over or formed, as though the XRD patterns are similar, VO₂ (B) shows its strongest intensity at the (110) peak, whereas V₂O₅ exhibits the highest intensity at (001).⁵ The hydrothermally synthesised VO₂ (B) also displays sharp peaks, demonstrating superior crystallinity.^{6,7}

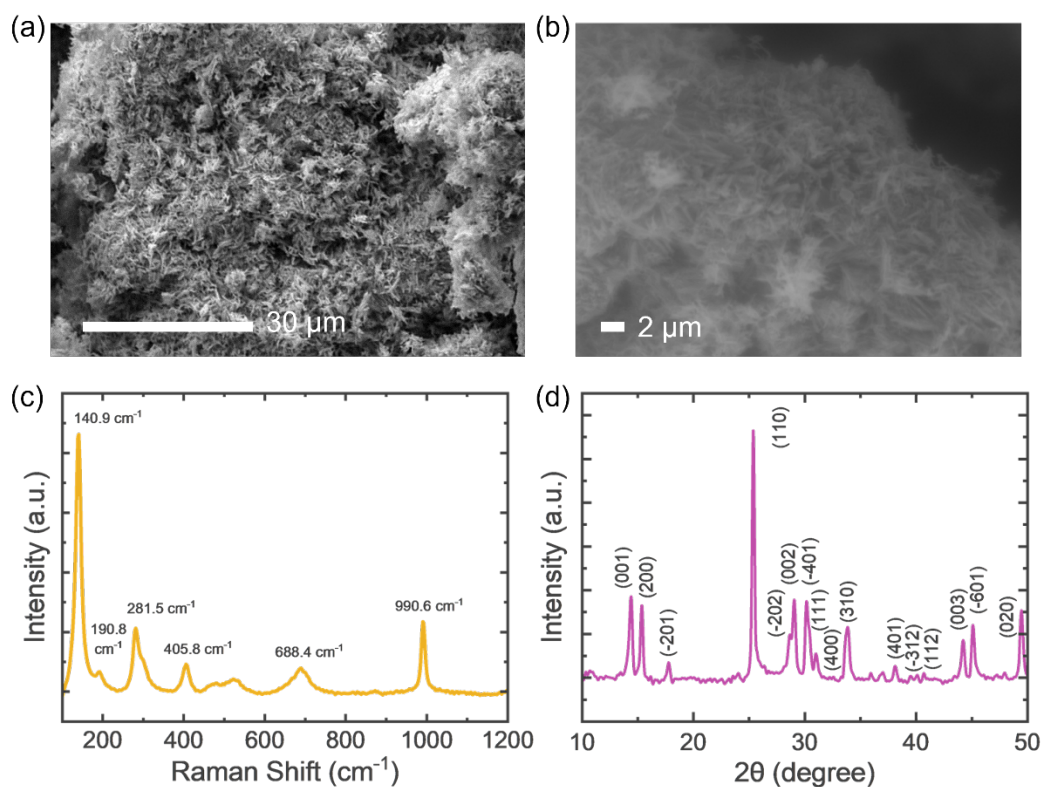


Figure S1. Characterisations of $\text{VO}_2(\text{B})$, cathode material; SEM images of $\text{VO}_2(\text{B})$ at (a) normal and (b) high magnification. (c) Raman spectrum and d) XRD spectrum.

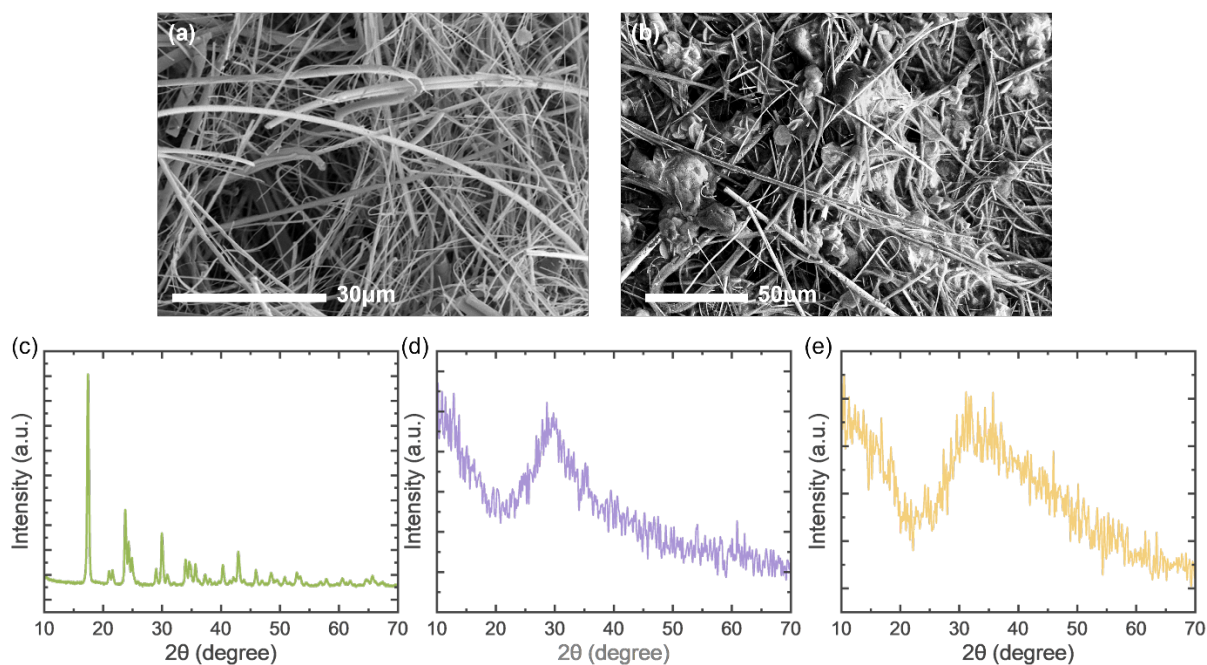


Figure S2. SEM images of (a) the pristine separator and (b) the separator with electrolyte used in the ZIBs assembled and tested. XRD spectra of (c) $\text{Zn}(\text{CF}_3\text{SO}_3)_2$ salt, (d) pristine separator and (e) separator with electrolyte solution dropped on top.

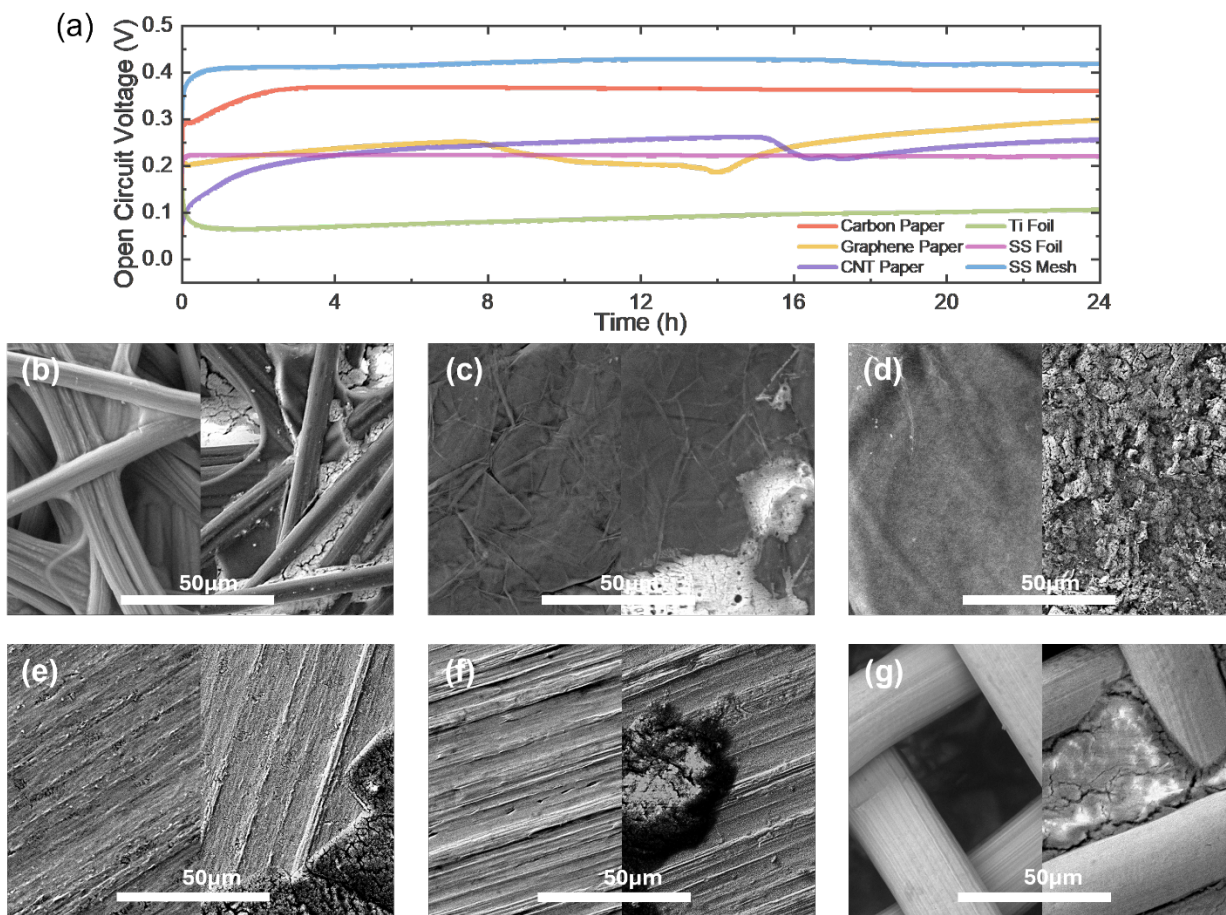


Figure S3. (a) OCV measurement of current collectors for 24 hours with no applied voltage. SEM images of the pristine current collectors before (left) and after (right) the measurement; (b) carbon paper, (c) graphene paper, (d) CNT paper, (e) titanium foil, (f) stainless steel foil and (g) stainless steel mesh.

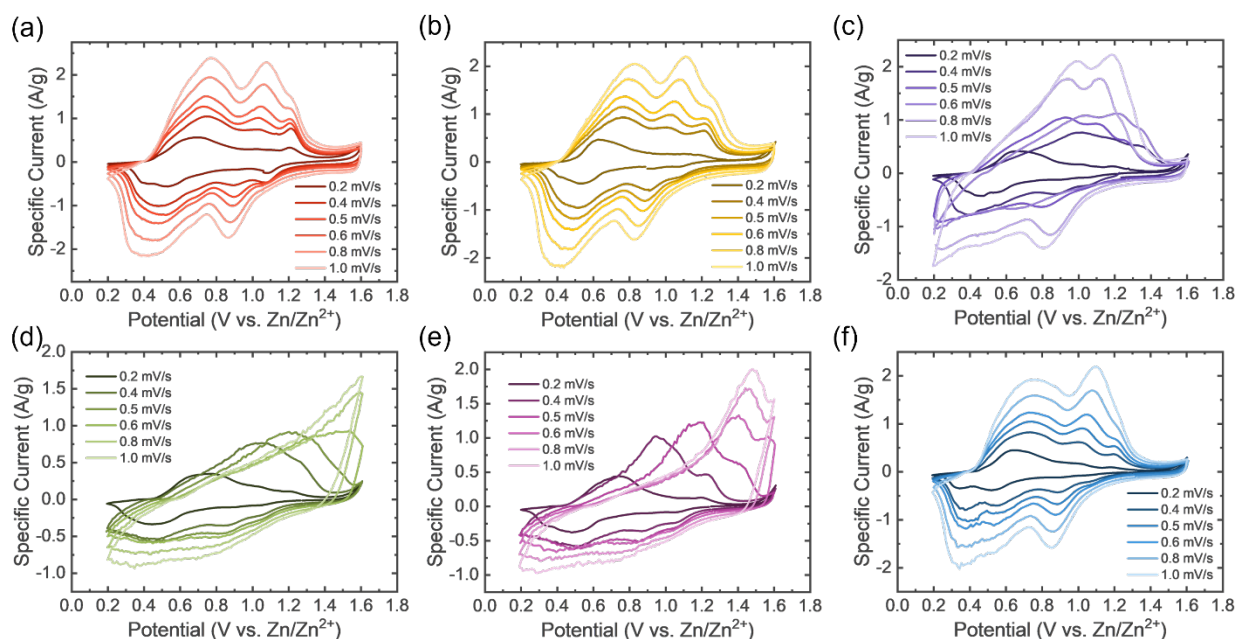


Figure S4. CV curves of each current collector; (a) carbon paper, (b) graphene paper, (c) CNT paper, (d) titanium foil, (e) stainless steel foil and (f) stainless steel mesh.

Current Collector Material	Capacity Retention
Carbon Paper	83.6%
Graphene Paper	40.0%
CNT Paper	0.00%
Titanium Foil	49.4%
Stainless Steel Foil	22.7%
Stainless Steel Mesh	93.3%

Table S1 – Capacity retention of cells with different current collectors after long term cycling for 1000 cycles at 2000 mA/g.

References

- 1 H. F. Xu, Y. Liu, N. Wei and S. W. Jin, *Optik (Stuttg)*, 2014, **125**, 6078–6081.
- 2 J. Chen, B. Xiao, C. Hu, H. Chen, J. Huang, D. Yan and S. Peng, *ACS Appl Mater Interfaces*, 2022, **14**, 28760–28768.
- 3 MDI Materials Data, 2019, preprint, Pro.
- 4 B. R. An, G. D. Lee, D. H. Son, S. H. Lee and S. S. Park, *Applied Chemistry for Engineering*, 2013, **24**, 611–615.
- 5 C. Londoño Calderón, C. Vargas Hernandez and J. Jurado, *Revista Mexicana de Fisica*, 2010, **56**, 411–415.
- 6 B. Deka Boruah, A. Mathieson, S. K. Park, X. Zhang, B. Wen, L. Tan, A. Boies and M. De Volder, *Adv Energy Mater*, 2021, **11**, 2100115.
- 7 S. Milošević, I. Stojković, S. Kurko, J. G. Novaković and N. Cvjetičanin, *Ceram Int*, 2012, **38**, 2313–2317.